Experimental Demonstration of a Balanced Electroabsorption Modulated Microwave Photonic Link

Sagi Mathai, *Student Member, IEEE*, Federica Cappelluti, Thomas Jung, *Student Member, IEEE*, Dalma Novak, *Member, IEEE*, Rodney B. Waterhouse, *Member, IEEE*, Deborah Sivco, Alfred Y. Cho, *Fellow, IEEE*, Giovanni Ghione, *Senior Member, IEEE*, and Ming C. Wu, *Senior Member, IEEE*

***Abstract*—A novel balanced electroabsorption modulated photonic link for simultaneous suppression of even-order distortions, third-order distortions, laser relative intensity noise (RIN), and common amplified spontaneous emission noise at the same modulator bias point was experimentally demonstrated for the first time. By biasing the balanced electroabsorption modulator at the third-order null, the third-order distortions were suppressed, while the balanced link architecture suppressed all even-order distortions and common mode noises. The fabricated balanced electroabsorption modulator (B-EAM) showed well-matched dc characteristics in terms of I–V and transfer curve. System experiments were performed to compare Single-EAM and B-EAM links. In the B-EAM link, 2-dB suppression of laser RIN and 20-dB improvement in spurious free dynamic range over the single-EAM link were observed.**

***Index Terms*—Balanced fiber-optic links, distortion suppression, electroabsorption modulator, intermodulation distortion, microwave photonics, relative intensity noise suppression.**

I. Introduction

DUE TO THE benefits of optical fiber (low loss, electromagnetic immunity, light weight, and ultrawide bandwidth), microwave photonic links are attractive for applications in antenna remoting, optical control of phased array antennas, fiber-radio, and cable television distribution. These applications possess stringent requirements in terms of link gain, noise figure (NF), and spurious free dynamic range (SFDR). To meet these demands, external intensity modulated direct detection links have been employed. Among these, balanced links are attractive due to their ability to simultaneously improve SFDR and NF by suppressing all even-order distortions, laser relative intensity noise (RIN), and common amplified spontaneous emission (ASE) noise. Shot-noise-limited performance can be achieved and, therefore, with increasing laser power, link gain and NF improve dramatically [1]–[3].

Conventional balanced links employ $LiNbO_3$ cross-coupled Mach–Zehnder modulators (X-MZM). The X-MZM must be biased at quadrature to enable balanced outputs (equal dc intensities and 180° out-of-phase modulated signals). Due to the sinusoidal behavior of its transfer curve, operating the X-MZM in balanced mode suppresses the second-order distortions, but maximizes the third-order distortions. Although system performance improves in terms of NF due to laser RIN suppression, the third-order distortions remain and limit the SFDR.

As a solution to this dilemma, we propose a novel balanced electroabsorption modulated photonic link which simultaneously suppresses laser RIN, common ASE noise, and all even-order distortions independent of the applied bias, as well as nulling of the third-order distortions. Electroabsorption modulators (EAMs) are attractive due to their small size, ultrawide bandwidth [4], low V_{π} [5], and their ability to be integrated with semiconductor optical amplifiers (SOAs) and distributed feedback (DFB) lasers [6]. Much effort has been focused on linearizing the EAM transfer curve. The developed techniques include electronic predistortion [7], distortion emulation and reversal [8], feed-forward compensation [9], RF current modulation [10], exploitation of the wavelength dependence of the quantum-confined Stark shift [11], dual-EAM approach [12], tailoring of the absorption coefficient along the propagation direction [13], and linearly combining the Franz–Keldysh and quantum-confined Stark effects [14], but these techniques cannot simultaneously suppress laser RIN or common ASE noise.

Previously, we experimentally demonstrated a monolithically integrated balanced electroabsorption modulator (B-EAM) [15], and theoretically analyzed the B-EAM link performance in terms of NF and SFDR [16]. In this paper, we experimentally demonstrate improvements in the B-EAM device characteristics and, for the first time, simultaneously suppress RIN, second-order distortions, and third-order distortions at the same bias point.

The paper is organized as follows. Section II explains the device operating principle, structure, and fabrication, and Section III describes our balanced link test bed and reports on some experimental results.

Manuscript received January 22, 2001; revised May 26, 2001. This work was supported in part by the ONR MURI on RF Photonic Materials and Devices under Contract N00014-97-10508 and by the UC MICRO Program under Project 98-186.

S. Mathai, T. Jung, and M. C. Wu are with the Electrical Engineering Department, University of California at Los Angeles, Los Angeles, CA 90095-1594 USA.

F. Cappelluti and G. Ghione are with Dipartimento di Elettronica, Politecnico di Torino, 10129 Turin, Italy.

D. Novak is with the Australian Photonics Cooperative Research Centre and the Department of Electrical and Electronic Engineering, University of Melbourne, Melbourne, Vic. 3052, Australia.

R. B. Waterhouse is with the Australian Photonics Photonics Cooperative Research Centre and the Department of Communication and Electronic Engineering, RMIT University, Melbourne, Vic. 3001, Australia.

D. Sivco and A. Y. Cho are with Lucent Technologies, Murray Hill, NJ 07974 USA.

Publisher Item Identifier S 0018-9480(01)08717-8.

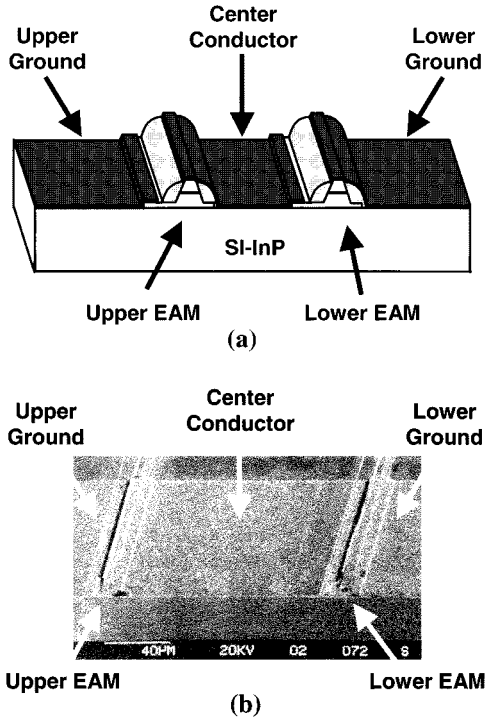

Fig. 1. B-EAM. (a) Device schematic. (b) SEM of a fabricated B-EAM. The B-EAM consists of a pair of EAMs monolithically integrated with a CPW transmission line on SI–InP. The center conductor connects the p-contact of the upper EAM to the n-contact of the lower EAM.

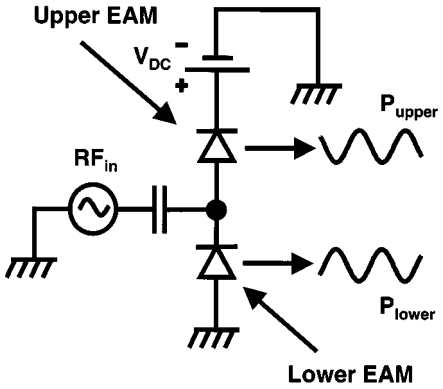

Fig. 2. Device principle: dc bias is applied in series, while the RF signals feed the center conductor. The B-EAM outputs are balanced independent of dc bias.

II. B-EAM

A. Device Structure and Link Operating Principle

Fig. 1 depicts the schematic structure and scanning electron micrograph (SEM) of a fabricated B-EAM, which consists of a pair of pin waveguide EAMs monolithically integrated with a coplanar waveguide (CPW) transmission line on semi-insulating (SI) InP. The center conductor connects the p-contact of the upper EAM to the n-contact of the lower EAM. To operate the device in balanced mode (Fig. 2), dc bias is applied between the two ground electrodes of the CPW, and the RF signals are applied between the center conductor and ground electrodes via a custom CPW probe with an integrated dc block and dc biasing terminal. Unlike the X-MZM, the outputs of the B-EAM are always balanced, independent of the bias voltage. Due to this unique ability, we may leverage on the balanced link's ability to suppress laser RIN, common ASE noise, and all-even order distortions without placing any restrictions on the modulator's bias point. Therefore, a balanced electroabsorption modulated photonic link can simultaneously suppress laser RIN, common ASE noise, all even-order distortions, and third-order distortions. Shot-noise-limited performance, ultralow NF, and fifth-order distortion limited SFDR can be simultaneously attained.

B. Device Fabrication

The epitaxial layers were grown by molecular beam epitaxy (MBE) on SI–InP. The waveguide structure consisted of a large InAlGaAs core with a thin bulk InAlGaAs ($\lambda_g = 1480$ nm) active region and InAlGaAs cladding layers [17]. InAlGaAs setback layers were incorporated to prevent dopant diffusion into the active layer during MBE growth. Highly doped InGaAs layers were used for the top and bottom p- and n-contact layers, respectively.

A double mesa structure was fabricated by wet etching to form an index-guided waveguide and allow access to the lower InGaAs ohmic contact layer. To bury the waveguide, passivate the sidewalls, reduce parasitic capacitance, and provide a dielectric bridge to interconnect the CPW transmission line with the top ohmic contact, photosensitive benzocyclobutane (Photo-BCB) was spun-on and patterned by optical lithography and subsequent development. It was hardcured in an oven set to 400 °C for 30 min. To expose the top p-contact for self-aligned metallization, the patterned Photo-BCB was dry etched with $CF_4 : O_2$ (4 : 1) plasma. n- and p-type alloyed ohmic contacts and the CPW transmission line were individually formed by electron beam evaporation and liftoff process. Finally, a brief rapid thermal annealing step was included to ensure activation of the ohmic contacts.

III. Experimental Results

A. B-EAM Electrical and Optical Characteristics

Fig. 3 shows the balanced-mode dc transfer curve for a B-EAM with 9×250 μm^2 waveguide dimensions and the I–V trace for each individual EAM. Both the normalized transfer curve and I–V trace showed well-matched behavior. The dark current level was 100 nA and the breakdown voltage was ~7 V. To measure the balanced mode dc transfer curve, an external-cavity tunable laser (ECTL) (1550-nm wavelength and 0- dBm optical power incident on each EAM) and two dc power supplies were required. Power supply 1 applied a 4-V reverse bias between the CPW upper and lower ground conductors. Power supply 2 was placed across the lower EAM and its voltage was swept from 0 to 4 V. The resulting fiber-to-fiber transmitted optical power was measured using an optical power sensor. The balanced-mode dc transfer curve shows improved complementary behavior than previously reported in [15]. The 0-V fiber-to-fiber insertion loss for the upper and lower EAM's was 14 dB, and the extinction ratio at 4-V bias was 8 dB. Applying the definition given in [18], the equivalent V_π for the upper and lower EAMs was 8 V. It should be mentioned that the current device has not been optimized for low V_π or insertion

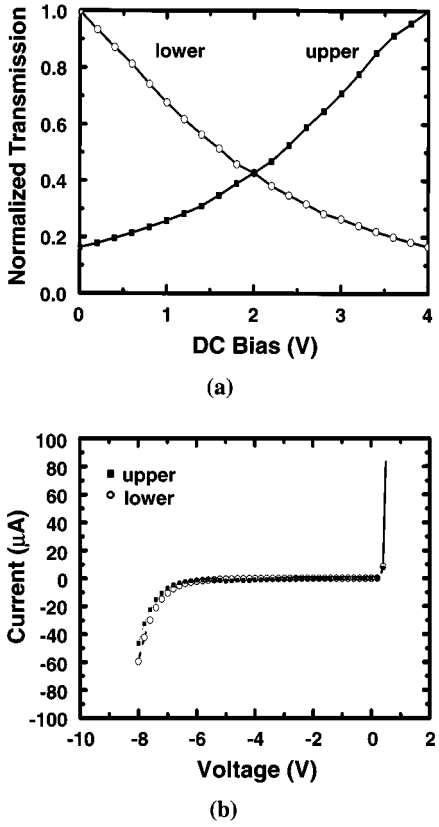

Fig. 3. B-EAM dc characteristics. (a) Normalized balanced-mode dc transfer curve. (b) I–V curves of the upper and lower EAMs in a B-EAM with 9×250 μm^2 waveguides. Well-matched characteristics were observed.

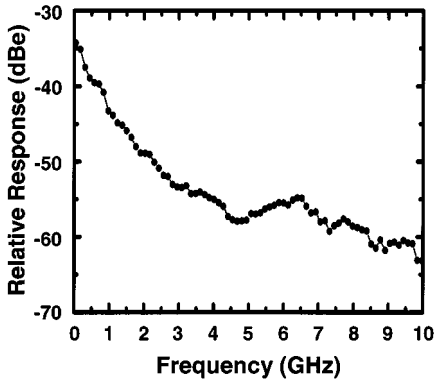

Fig. 4. Electrical frequency response. A single-EAM in a B-EAM with 16×300 μm^2 waveguides was tested. The *RC* limited bandwidth was 310 MHz at 2-V bias.

loss. Due to accidental damage to the above-mentioned device, we switched to a B-EAM with 16×300 μm^2 waveguides for the remainder of the experiments. All system level experiments and frequency response measurements were performed with the wider waveguide B-EAM.

Fig. 4 depicts the S_{21} parameter measured with a vector network analyzer and lightwave test set for the lower arm of the B-EAM. A shunt resistor or termination was not employed. Ten dBm of optical power was incident on each EAM from the ECTL. The measured electrical 3-dB bandwidth was 310 MHz at 2-V bias. The low frequency response was caused by the large

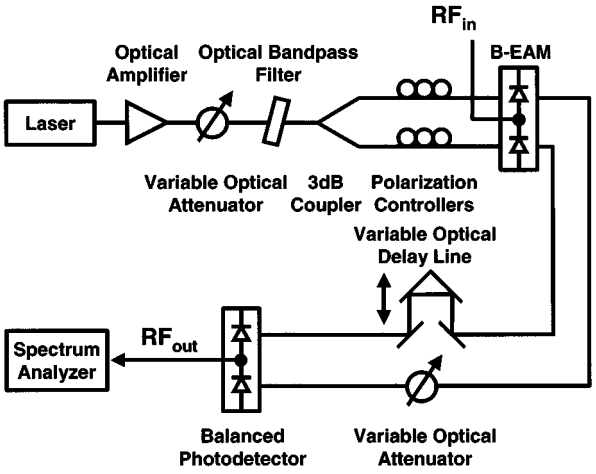

Fig. 5. Balanced link testbed.

capacitance (calculated to be 3.8 pF per EAM) from the pair of EAMs. Higher bandwidth can be achieved by reducing the width and length of the EAMs.

B. B-EAM Link Test Bed

Fig. 5 illustrates the B-EAM experimental setup. The driving microwave signals were pre-amplified and low-pass-filtered prior to feeding the modulator. An optical delay line and variable optical attenuator on the upper and lower output arms compensated for RF phase and amplitude mismatch, respectively. A 10-GHz balanced photodetector received the modulated optical signals, and a 50-GHz spectrum analyzer monitored them. This setup was also used to test Single-EAM links by disconnecting one fiber arm to the balanced receiver.

A monolithic approach can be employed to reduce the transmitter complexity and improve the phase stability of the link. On the input side of the B-EAM, a DFB laser and a Y-branch or multimode interference coupler may be employed.

On the output side, polarization multiplexing can be exploited to reduce the fiber count to one. Polarization rotators, splitters, and multiplexers have been monolithically integrated on InP [19].

C. System Performance

To demonstrate RIN suppression, a DFB laser with 1543-nm wavelength was employed as the optical source. The laser output was amplified by an erbium-doped fiber amplifier (EDFA) and filtered by an optical bandpass filter to remove excess ASE. The bias on the DFB laser was adjusted to maximize the RIN peak, which occurred at 910 MHz. The optical power was increased until RIN dominated the noise floor. To verify this, the optical power was increased by 3 dB, which resulted in a 6-dB increase in the RIN spectrum. The bias on the modulator was set to 0 V. Fig. 6 shows the measured RIN spectrum passing through a Single-EAM and B-EAM. The total detected dc photocurrent for the Single-EAM and B-EAM links was 540 μA and 1.093 mA (including upper and lower arms), respectively. RIN suppression greater than 10 dB from dc to 1 GHz was achieved with the B-EAM link. At higher frequencies, fiber path length

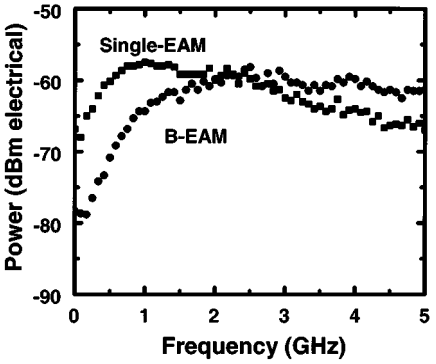

Fig. 6. RIN spectrum for the single and B-EAM's links: in the B-EAM link, RIN was suppressed by more than 10 dB from dc to 1 GHz.

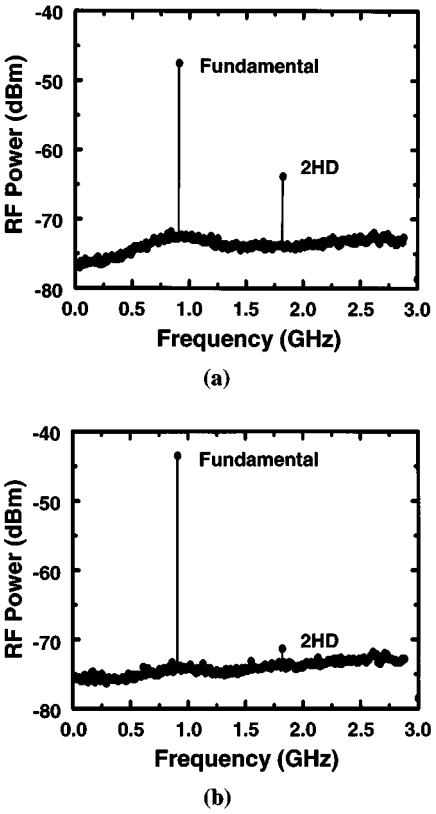

Fig. 7. Simultaneous RIN and distortion suppression. (a) Single-EAM. (b) B-EAM. The fundamental frequency was set to the RIN peak (910 MHz), while the 2HD lied at 1.82 GHz. In the B-EAM link, the 2HD and RIN were suppressed by 7.5 and 2 dB, respectively.

matching becomes more stringent. By improving the phase mismatches in the link, RIN suppression can be achieved over a wider bandwidth.

To demonstrate simultaneous RIN and distortion suppression, the B-EAM was modulated at the RIN peak (910 MHz). The total incident optical and RF powers on the B-EAM were set to 14 and 10 dBm, respectively. The third-order harmonic was suppressed by adjusting the modulator's bias voltage, while the second-harmonic distortion (2HD) was suppressed by compensating for any amplitude and phase mismatch with the optical attenuator and delay line, respectively. Fig. 7 contains the spectrum analyzer traces showing the fundamental 910-MHz signal and the 1.82-GHz 2HD for the Single-EAM and B-EAM links.

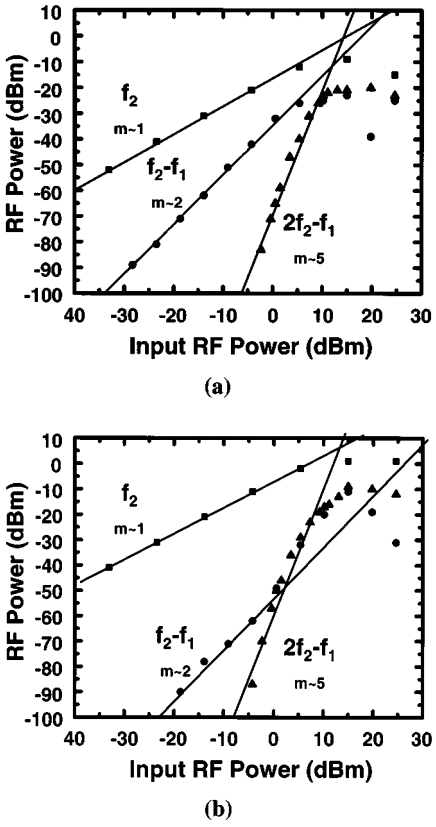

Fig. 8. Two-tone measurement. (a) Single-EAM. (b) B-EAM. In both cases, $f_2 = 150$ MHz, $f_2 - f_1 = 30$ MHz, and $2f_2 - f_1 = 180$ MHz. In the B-EAM link, the second-order distortion $(f_2 - f_1)$ was suppressed by 17 dB, and assuming a thermal noise-limited noise floor (-174 dBm/Hz), we observed 20-dB improvement in SFDR.

In the balanced case, the 2HD and RIN were suppressed by 7.5 and 2 dB at the RIN peak, respectively. The device used in this experiment had an insertion loss of 20 dB at 0-V bias. Much higher RIN suppression can be achieved via optimization of the fiber-to-fiber insertion loss through the B-EAM.

To examine the microwave linearity of the link, we performed a two-tone measurement. One microwave synthesizer was set to 120 MHz (f_1) and the other to 150 MHz (f_2). These signals were pre-amplified and low-pass-filtered prior to driving the modulator. We replaced the DFB laser with an ECTL set to 1550 nm. After optical amplification and bandpass filtering, the laser power incident on the upper and lower EAM was 10 dBm. The modulator bias was set to null the third-order distortion and the link was balanced to suppress second-order distortions. The total dc photocurrent in the Single-EAM and B-EAM links was 4.5 μA and 21.2 μA (upper plus lower arm). An RF amplifier with 52 dB of gain was employed to amplify the detected RF signals. Fig. 8 depicts the signal power plot of the Single-EAM and B- EAM links. In both links, the intermodulation distortion $(2f_2 - f_1)$ had a fifth-order RF power dependence. Although in the B-EAM link, the second-order distortion $(f_2 - f_1)$ was suppressed by 17 dB, it limited the SFDR. Assuming a thermal noise limited noise floor (-174 dBm/Hz), the broad-band SFDR was calculated to be 83 and 63 dB$\cdot$Hz$^{1/2}$ for the B-EAM and Single-EAM links, respectively. Twenty decibels of improvement in SFDR was observed for the B-EAM

link over the Single-EAM link, while the actual improvement due to the balanced link alone (assuming equal output RF signal powers) was estimated to be 14.5 dB. Optimizing the B-EAM for low insertion loss and improving the phase mismatches in the experimental setup can result in much higher SFDR.

We modeled a B-EAM link using our previously reported theory [16]. For a total received laser power of 10 mW, a RIN level of -140 dBc/Hz, and a B-EAM with a V_π of 0.5 V and 10-dB insertion loss, we predict that a shot-noise fifth-order distortion-limited SFDR of 130 dB$\cdot$Hz$^{4/5}$ can be achieved.

IV. Conclusion

Utilizing a novel balanced electroabsorption modulator, we have successfully demonstrated, for the first time, simultaneous suppression of second-order distortion, third-order distortion, and laser RIN at the same modulator bias point. We have reviewed the device principle and fabrication technique, and performed both dc and RF characterization. A comparison between Single-EAM and B-EAM links was provided to highlight the innovative capabilities of the B-EAM. By biasing the B-EAM at the third-order null and operating the link in balanced mode, 7.5-dB suppression of second-order distortion, and 2-dB suppression of laser RIN at the RIN peak (910 MHz) was experimentally demonstrated. The two-tone measurement showed 17-dB suppression of second-order distortion and 20-dB improvement in SFDR compared to the Single-EAM link. With optimization of the device design to improve insertion loss, V_π, and bandwidth, as well as matching of the optical path lengths in the experimental setup, ultrawide SFDR and ultralow NF can be achieved.

Acknowledgment

The authors would like to thank Dr. T. Chau, Tellium Inc., Oceanport, NJ, and Dr. S. Islam, Gazillion Bits Inc., San Jose, CA, for their guidance during their stay at UCLA.

References

[1] K. J. Williams and R. D. Esman, "Optically amplified downconverting link with shot noise limited performance," *IEEE Photon. Technol. Lett.*, vol. 8, pp. 148–150, Jan. 1996.

[2] E. Ackerman, S. Wanuga, J. MacDonald, and J. Prince, "Balanced receiver external modulation fiber-optic link architecture with reduced noise figure," in *IEEE MTT-S Int. Microwave Symp. Dig.*, vol. 2, June 1993, pp. 723–726.

[3] M. S. Islam, T. Chau, S. Mathai, T. Itoh, M. C. Wu, D. L. Sivco, and A. Y. Cho, "Distributed balanced photodetectors for broad-band noise suppression," *IEEE Trans. Microwave Theory Tech.*, vol. 47, pp. 1282–1287, July 1999.

[4] T. Ido, S. Tanaka, M. Suzuki, M. Koizumi, H. Sano, and H. Inoue, "Ultra-high-speed multiple-quantum-well electro-absorption optical modulators with integrated waveguides," *J. Lightwave Technol.*, vol. 14, pp. 2026–2034, Sept. 1996.

[5] K. K. Loi, J. H. Hodiak, X. B. Mei, C. W. Tu, W. S. C. Chang, D. T. Nichols, L. J. Lembo, and J. C. Brock, "Low-loss 1.3-μm MQW electroabsorption modulators for high-linearity analog optical links," *IEEE Photon. Technol. Lett.*, vol. 10, pp. 1572–1574, Nov. 1998.

[6] N. Souli, A. Ramdane, F. Devaux, A. Ougazzaden, and S. Slempkes, "Tandem of electroabsorption modulators integrated with a DFB laser and an optical amplifier for short optical pulse generation and coding," *Proc. Inst. Elect. Eng.*, pt. J, vol. 145, pp. 198–204, June 1998.

[7] Y. Chiu, B. Jalali, S. Garner, and W. Steier, "Broad-band electronic linearizer for externally modulated analog fiber-optic links," *IEEE Photon. Technol. Lett.*, vol. 11, pp. 48–50, Jan. 1999.

[8] J. Yu, T. Y. Chang, G. C. Wilson, T. H. Wood, N. J. Sauer, J. E. Johnson, T. Tanbun-Ek, and P. A. Morton, "Linearization of 1.55-μm electroabsorption modulated laser by distortion emulation and reversal for 77-channel CATV transmission," *IEEE Photon. Technol. Lett.*, vol. 10, pp. 433–435, Mar. 1998.

[9] T. Iwai, K. Sato, and K. Suto, "System distortion and noise in AM-SCM transmission systems employing the feedforward linearized MQW-EA external modulator," *J. Lightwave Technol.*, vol. 13, pp. 1606–1612, Aug. 1995.

[10] G. C. Wilson, T. H. Wood, and U. Koren, "Integrated electroabsorption modulator/DBR laser linearized by RF current modulation," *IEEE Photon. Technol. Lett.*, vol. 7, pp. 1154–1156, Oct. 1995.

[11] K. K. Loi, J. H. Hodiak, X. B. Mei, C. W. Tu, and W. S. C. Chang, "Linearization of 1.3-μm MQW electroabsorption modulators using an all-optical frequency-insensitive technique," *IEEE Photon. Technol. Lett.*, vol. 10, pp. 964–966, July 1998.

[12] G. W. Lee and S. K. Han, "Wideband linear analog modulation using dual electroabsorption modulator," in *CLEO/Pacific Rim Tech. Dig.*, vol. 2, Aug. 1999, pp. 195–196.

[13] C. H. Lee and S. K. Han, "Linearity enhancement of electroabsorption optical modulator by absorption variation in propagation direction," *Microwave Opt. Technol. Lett.*, vol. 22, pp. 30–35, July 1999.

[14] R. B. Welstand, J. T. Zhu, W. X. Chen, A. R. Clawson, P. K. L. Yu, and S. A. Pappert, "Combined Franz–Keldysh and quantum-confined Stark effect waveguide modulator for analog signal transmission," *J. Lightwave Technol.*, vol. 17, pp. 497–502, Mar. 1999.

[15] S. Mathai, T. Jung, F. Cappelluti, D. Novak, R. Waterhouse, G. Ghione, D. Sivco, A. Y. Cho, and M. C. Wu, "Experimental demonstration of a balanced electroabsorption modulator," in *Int. Microwave Photon. Topical Meeting Tech. Dig.*, Sept. 2000, pp. 9–12.

[16] F. Cappelluti, S. Mathai, G. Ghione, and M. C. Wu, "High performance RF photonic link using a balanced electroabsorption modulator," in *Proc. Photon. Syst. Antenna Arrays*, Feb. 2000, Session 3.

[17] M. K. Chin and W. S. C. Chang, "InGaAs/InAlAs quantum-well electroabsorption waveguide modulators with large core waveguide structure: Design and characterization," *Appl. Opt.*, vol. 34, pp. 1544–1553, Mar. 1995.

[18] R. B. Welstand, S. A. Pappert, D. T. Nichols, L. J. Lembo, Y. Z. Liu, and P. K. L. Yu, "Enhancement in electroabsorption waveguide modulator slope efficiency at high optical power," *IEEE Photon. Technol. Lett.*, vol. 10, pp. 961–963, July 1998.

[19] U. Hilbk, T. Hermes, P. Meissner, F. J. Westphal, G. Jacumeit, R. Stenzel, and G. Unterbörsch, "First system experiments with a monolithically integrated tunable polarization diversity heterodyne receiver OEIC on InP," *IEEE Photon. Technol. Lett.*, vol. 7, pp. 129–131, Jan. 1995.

Sagi Mathai (S'97) received the B.S. and M.S. degrees in electrical engineering from the University of California at Los Angeles (UCLA), in 1997 and 2001, respectively, and is currently working toward the Ph.D. degree in electrical engineering at UCLA.

He conducts research in the area of microwave photonics and high-speed integrated optoelectronics. He has authored or co-authored 20 technical papers in these fields.

Mr. Mathai is a member of the Optical Society of America and Eta Kappa Nu.

Federica Cappelluti was born in Ortona, Italy, in 1973. She received the Laurea degree in electronic engineering from the Politecnico di Torino, Turin, Italy, in 1998, and is currently working toward the Ph.D. degree in electronic engineering at the Politecnico di Torino.

Her research interests have included design, fabrication, and characterization of passive integrated devices for optical communication applications. Her current research interests concern the simulation, modeling and design of high-speed electroabsorption modulators and photodiodes, and their system application in high-performance fiber-optic links. She is also involved in the thermal modeling of active microwave devices.

Thomas Jung (S'96) received the B.S. and M.S. degrees in electrical engineering from the University of California at Los Angeles (UCLA), in 1996 and 1998, respectively, and is currently working toward the Ph.D. degree in electrical engineering at UCLA.

His research interests are electrooptic sampling of high-speed photonic devices, ultrafast lasers, RF photonics, and device modeling of photonic devices.

Dalma Novak (S'90–M'91) received the Bachelor of Engineering (electrical) (with first-class honors) and the Ph.D. degree from the University of Queensland, Brisbane, Australia, in 1987 and 1992, respectively.

In 1992, she joined the Photonics Research Laboratory (PRL), Department of Electrical and Electronic Engineering, The University of Melbourne, Melbourne, Australia, where she is currently an Associate Professor and Reader. She is also a Key Researcher at the Australian Photonics Cooperative Research Centre (CRC) and Deputy Director of the PRL. She has authored or co-authored over 120 papers in these areas. Her research interests include fiber-wireless communication systems, semiconductor lasers, and high-speed optical networks.

Rodney B. Waterhouse (S'90–M'94) received the B.E. (Hons), M.Eng.Sc. (Research), and Ph.D. degrees from the University of Queensland, Brisbane, Australia, in 1987, 1990, and 1994, respectively.

In 1994, he joined the School of Electrical and Computer Engineering, RMIT University, Melbourne, Australia, where he is currently a Senior Lecturer. His research interests include printed antennas, phased arrays, optically distributed wireless systems, and photonic devices for microwave applications. He has authored or co-authored more than 130 papers and holds three patents in these areas. In 2000, RMIT University became a member of the Australian Photonics Cooperative Research Centre (CRC), where he is currently a CRC Key Researcher. From mid-2000 to the beginning of 2001, he was a Visiting Professor with the Department of Electrical Engineering, University of California at Los Angeles, for three months and then a Visiting Researcher in the Photonics Technology Branch, Naval Research Laboratories, Washington, DC, for an additional three months while on his sabbatical.

Dr. Waterhouse is the former chair of the IEEE Victorian Microwave Theory and Techniques Society (MTT-S)/Antennas and Propagation Society (AP-S) Chapter.

Deborah Sivco, photograph and biography not available at the time of publication.

Alfred Y. Cho (S'57–M'60–SM'79–F'81), photograph and biography not available at the time of publication.

Giovanni Ghione (M'87–SM'94) was born in Alessandria, Italy, in 1956. He received the degree in electronic engineering (*cum laude)* from the Politecnico di Torino, Turin, Italy, in 1981.

In 1983, he became a Research Assistant with the Politecnico di Torino. From 1987 to 1990, he was an Associate Professor with the Politecnico di Milano, Milan, Italy. In 1990, he joined the University of Catania as a Full Professor of Electronics. Since 1991 he has held the same position at the Politecnico di Torino II, Faculty of Engineering. Since 1981, he has been engaged in Italian and European research projects (ESPRIT 255, COSMIC and MANPOWER) in the field of active and passive microwave computer-aided design (CAD). His current research interests concern the physics-based simulation of active microwave and optoelectronic devices, with particular attention to noise modeling, thermal modeling, and active device optimization. His research interests also include several topics in computational electromagnetics, including coplanar component analysis. He has authored or co-authored more than 150 papers and book chapters in the above fields.

Prof. Ghione is member of the Editorial Board of the IEEE TRANSACTIONS ON MICROWAVE THEORY AND TECHNIQUES and is a member of the Associazione Elettrotecnica Italiana (AEI).

Ming C. Wu (S'82–M'83–SM'00) received the M.S. and Ph.D. degrees in electrical engineering from the University of California at Berkeley, in 1985 and 1988, respectively.

From 1988 to 1992, he was a Member of Technical Staff at AT&T Bell Laboratories, Murray Hill, NJ, where he conducted research in high-speed semiconductor lasers and optoelectronics. In 1993, he joined the faculty of the Electrical Engineering Department, University of California at Los Angeles (UCLA), where he is currently a Professor. He has authored or co-authored over 100 journal papers, 180 conference papers, contributed one book chapter, and holds eight U.S. patents. His current research interests include microelectromechanical systems (MEMS), microoptical electromechanical systems (MOEMS), ultrafast integrated optoelectronics, microwave photonics, high-power photodetectors, and modulators.

Dr. Wu is a member of the American Physical Society, the Optical Society of America, the International Scientific Radio Union (URSI), and Eta Kappa Nu. He is the director of the Multiuniversity Research Initiative (MURI) Center on RF Photonic Materials and Devices sponsored by the Office of Naval Research (ONR) and a member of the California NanoSystem Institute (CNSI). He was general co-chair of the IEEE Lasers and Electro-Optics Society (IEEE LEOS) Summer Topical Meeting in 1995 (RF Optoelectronics), 1996 and 1998 [Optical Microelectromechanical Systems (MEMS)], and 1998 International Conference on MOEMS. He has also served on the Program Committees of the Optical Fiber Communication Conference (OFC), Conference on Lasers and Electro Optics (CLEO), MEMS, Optical MEMS, International Electron Device Meeting (IEDM), and Device Research Conference (DRC). He was the recipient of the 1992 Packard Foundation Fellowship and the 1994 Meritorious Conference Paper Award of the Government Microcircuit Applications Conference (GOMAC).